

See discussions, stats, and author profiles for this publication at: <https://www.researchgate.net/publication/283560740>

Cell Chemistry of Sodium–Oxygen Batteries with Various Nonaqueous Electrolytes

ARTICLE *in* THE JOURNAL OF PHYSICAL CHEMISTRY C · OCTOBER 2015

Impact Factor: 4.77 · DOI: 10.1021/acs.jpcc.5b09187

READS

14

2 AUTHORS, INCLUDING:



Xiangxin Guo

Chinese Academy of Sciences

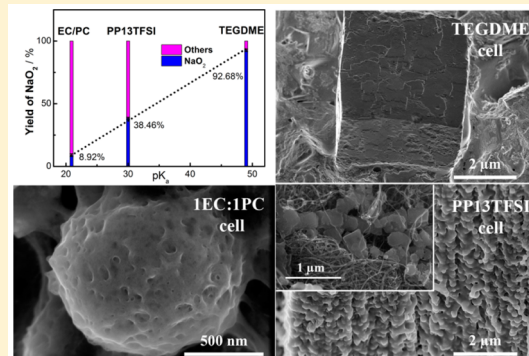
64 PUBLICATIONS 596 CITATIONS

[SEE PROFILE](#)

Cell Chemistry of Sodium–Oxygen Batteries with Various Nonaqueous Electrolytes

Ning Zhao^{†,‡} and Xiangxin Guo^{*,†}[†]State Key Laboratory of High Performance Ceramics and Superfine Microstructure, Shanghai Institute of Ceramics, Chinese Academy of Sciences, 1295 Ding Xi Road, Shanghai 200050, China[‡]Graduate School of Chinese Academy of Sciences, Beijing 100039, China**S Supporting Information**

ABSTRACT: Development of the nonaqueous Na–O₂ battery with a high electrical energy efficiency requires the electrolyte stable against attack of highly oxidative species such as nucleophilic anion O₂^{•-}. A combined evaluation method was used to investigate the Na–O₂ cell chemistry with various solvents, including ethylene carbonate/propylene carbonate (EC/PC)-, *N*-methyl-*N*-propylpiperidinium bis(trifluoromethansulfonyl) imide (PP13TFSI)-, and tetraethylene glycol dimethyl ether (TEGDME)-based electrolytes. It is found that the TEGDME-based electrolytes have the best stability with the predominant yield of NaO₂ upon discharge and the largest electrical energy efficiency (approaching 90%). Both EC/PC- and PP13TFSI-based electrolytes severely decompose during discharge, forming a large amount of side products. Analysis of the acid dissociation constant (pK_a) of these electrolyte solvents reveals that the TEGDME has the relatively large value of pK_a , which correlates with good stability of the electrolyte and high round-trip energy efficiency of the battery.



INTRODUCTION

Rapid development of electric vehicle and large-scale stationary electricity storage requires batteries with higher energy densities than the currently used Li-ion batteries.^{1,2} Under such circumstance, metal–air batteries with metal anodes and oxygen cathodes have attracted considerable attention in recent years.^{3–5} Of these batteries, one of the most attractive is the Li–air (or Li–O₂) battery, which produces the crystalline lithium peroxide (Li₂O₂) particles for releasing energy and decomposes the formed Li₂O₂ for regaining the storage ability. In theory, the Li–O₂ battery may deliver a gravimetric energy density of 3458 Wh kg⁻¹ in the case of two electron reduction of O₂ and 5200 Wh kg⁻¹ in the case of four electron reduction of O₂.^{6–10} It nevertheless faces a number of critical challenges such as the stability of the electrolytes, the limited cycle life, and the low “round-trip” electrical energy efficiency (normally smaller than 80%).^{11,12} Though many efforts have been made to overcome the aforementioned problems, the electrical energy efficiency of the Li–O₂ battery is still far below 90%, even the cycle number being extended above 1000. Very interestingly, the recently reported Na–O₂ batteries exhibited small cycle overpotential (<0.2 V) with the result of electrical energy efficiency above 90%.^{13,14} This distinct difference implies that it is worthwhile clarifying the cell chemistry of Na–O₂ battery, which might be helpful for understanding and finding solutions to improve the electrical energy efficiency of the Li–O₂ battery.

In fact, the first reported Na–O₂ battery was constructed with the polymer electrolyte, which could be cycled for several times at 105 °C using the liquid sodium anode.¹⁵ In this work, identification of reaction products was lack. Later on, Fu et al. reported the Na–O₂ batteries with carbonate (ethylene carbonate and dimethyl carbonate, EC/DMC)- and ether (dimethoxyethane, DME)-based electrolytes.^{16,17} According to transmission electron microscopy (TEM) observation in local areas of the discharged cathodes, they stated that Na₂O₂ might be the major discharge product in both-type batteries. Nearly at the same time, Kang et al.¹⁸ studied the Na–O₂ batteries with both propylene carbonate (PC)- and tetraethylene glycol dimethyl ether (TEGDME)-based electrolytes. On basis of X-ray diffraction (XRD) and Fourier transform infrared (FTIR) measurements, they concluded that Na₂CO₃ was the dominant discharge product for the PC-based batteries and Na₂O₂·2H₂O was the counterpart for the TEGDME-based ones. NaO₂ as the dominant discharge product was first demonstrated in the rechargeable Na–O₂ batteries by Janek's group.¹³ They used diethylene glycol dimethyl ether (DEGDME)-based electrolytes, and the battery tests were carried out under a static pure oxygen atmosphere. The same discharge product (i.e., NaO₂) has also been identified in the Na–O₂ batteries with the TEGDME-based electrolytes in our previous work.¹⁹ According

Received: September 21, 2015

Revised: October 20, 2015

Published: October 20, 2015



ACS Publications

© 2015 American Chemical Society

25319

DOI: 10.1021/acs.jpcc.5b09187
J. Phys. Chem. C 2015, 119, 25319–25326

to the above discussion, it is obvious that the reaction mechanisms of Na–O₂ batteries are far from reaching an agreement. Different sodium oxides such as NaO₂, Na₂O₂, Na₂O₂·2H₂O, or Na₂CO₃ could be formed dependent on various electrolytes. Comprehensive characterizations of discharge products with respect to different electrolytes, especially in quantitative terms, is still needed.

Therefore, in this work, we selected different electrolytes that are conventionally used in the metal–air batteries and carried out investigations on their influence on the cathode reactions of the Na–O₂ batteries. Measurements of X-ray diffraction (XRD), scanning electron microscope (SEM), Raman spectroscopy, and Fourier transform infrared (FTIR) spectroscopy were conducted to study the crystallinity, morphology, and chemical composition of the discharge products. Furthermore, technique of NaO₂ titration was used to quantitatively analyze the amount of NaO₂ formed after the first discharge. The cell chemistry and underlying mechanism with respect to these various electrolytes are discussed.

EXPERIMENTAL SECTION

Cathode Preparation. Vertically aligned carbon nanotubes (VACNTs) grown on stainless steel (SS) networks (Microphase Co. LTD) were used as the air cathodes. Their structure and morphology are the same as those reported previously.¹¹ The carbon nanotubes are approximately 1.5 mg cm⁻² in mass with a specific surface area of approximately 80 m² g⁻¹ as measured by ASAP 2010. The average cathode area and mass were 0.5 cm² and 0.7 mg, respectively. The air cathodes were dried at 80 °C under vacuum for 48 h before battery assembly.

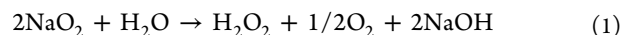
Electrolyte preparation. For preparing the electrolytes, the tetraethylene glycol dimethyl (TEGDME, Aldrich, ≥99.0%), propylene carbonate (PC, Aldrich, anhydrous, 99.7%), and ethylene carbonate (EC, Aldrich, anhydrous, 99.0%) were dried by freshly activated molecular sieves (4 Å type) for more than 1 week. The ionic liquid of PP13TFSI (Kanto Chemical Corporation) in battery grade was dried by baking at 80 °C for 48 h in vacuum. The final water content in each solvent was below 10 ppm measured by a Metrohm 831 KF Coulometer. The sodium triflate (NaSO₃CF₃, Aldrich, 98% trace metal basis) was prebaked at 80 °C in vacuum for 48 h. Then the electrolytes were made of each solvent dissolved with NaSO₃CF₃.

Cell Assembly and Operating Conditions. The Na–O₂ batteries were assembled in a glovebox with a circulation of high-purity Ar atmosphere. The content of H₂O as well as O₂ was maintained below 0.1 ppm. Each Swagelok-type cell was assembled in a vertical geometry with a Na foil, a glass fiber (Whatman) and a separator (Asahi Kasei Corporation) soaked with 80 μL electrolyte, and a VACNT cathode with the carbon nanotube side facing the gas atmosphere. The assembled batteries were transferred to an Ar/O₂ glovebox without exposure to ambient atmosphere. All the Na–O₂ batteries were tested under the static Ar/O₂ (80/20 vol %) atmosphere inside the glovebox with the level of moisture below 0.2 ppm. Detailed description on the construction of the glovebox used here (Vigor Gas Puri. Tech. Inc.) can be found in our previous report.¹⁹ The galvanostatic discharge/charge curves of the Na–O₂ batteries were measured by a cycle tester (Arbin BT2000) at room temperature. Before the measurement, the cells were rested for 4 h to reach the equilibrium open circuit voltage (i.e., 2.9 V). The current density of 0.1 mA cm⁻² applied here corresponds to 67 mA g⁻¹ according to the loading of carbon

nanotubes in the cathode (i.e., 1.5 mg cm⁻²). The specific capacity is normalized according to the mass of carbon nanotubes in the VACNT cathodes.

Characterization. The discharged VACNT cathodes were taken out from the cells in the argon glovebox, rinsed by anhydrous DME, and dried on a filter paper under vacuum. Afterward they were used for spectroscopy and morphology characterizations. The XRD measurement was carried out with a sample holder, which was sealed by two silicon-glue rings together with a stainless-steel plate and a Be window, a detailed description of which was given in ref 11b. The XRD scan was conducted using a diffractometer (D8 Discover, Bruker) with Cu K α radiation in a reflection mode. The morphologies of cathodes were studied by scanning electron microscope (SEM, FEI Magellan 400). Raman spectroscopy was performed using a HORIBA Jobin Yvon HR800 confocal microscope with the excitation wavelength of 514.53 nm. For this measurement, the discharged cathodes were protected with a homemade sample holder, which was sealed by two silicon-glue rings together with a stainless-steel plate and a quartz glass window. Fourier transform infrared (FTIR) spectroscopy data were collected with a FTIR spectrometer (Bruker Tensor 27), which was equipped with an attenuated total reflectance (ATR) accessory and settled in a glovebox filled with high-purity Ar atmosphere.

NaO₂ Titration Protocol. This method was proposed and developed by Hartmann et al.¹⁴ and McCloskey et al.,²⁰ which allows direct measurement of the amount of NaO₂ on the cathode after discharge. Briefly, the discharged VACNTs cathodes were extracted from cells with various electrolytes and were immersed in H₂O, where H₂O₂ would form from the reaction between NaO₂ and H₂O via



The resulting H₂O₂ was quantified using a standard iodometric titration.^{14,20} The yield of NaO₂ is defined as the amount of NaO₂ produced divided by the amount of NaO₂ expected given the Coulometry as referred to ref 21a. The detailed process is given in Supporting Information. Note that this protocol has proven to be valid in quantifying the amounts of Li₂O₂ formed in Li–O₂ batteries and NaO₂ in Na–O₂ batteries.^{21a,b}

pK_a Measurement. The acid dissociation constant (i.e., pK_a) was the C–H acidity constant of a nonaqueous solvent in an aprotic environments. The solvent's stability against the O₂^{•-} attack significantly depends on the pK_a in its own environment. The measurement of pK_a values in DMSO have been extensively conducted by a UV–vis spectroscopic method because DMSO is reasonably stable against O₂^{•-}. This method was first proposed and developed by Bordwell et al.²⁰ The experimental process was briefly described in Supporting Information.

RESULTS AND DISCUSSION

To examine influence of various electrolytes on cell chemistry of the Na–O₂ batteries, we chose EC/PC (1:1 vol %) for representing the alkyl carbonate solvents, TEGDME for the ether,^{22a–c} and PP13TFSI for the ionic liquid.^{22d} We also tried the dimethyl sulfoxide (DMSO)-based electrolyte, which was commonly used for the aprotic Li–O₂ battery in literature.^{22e} However, it is found that the DMSO-based electrolytes severely react with the sodium metal anode. Thus, here we focus on the electrolytes that are relatively stable against the sodium metal anode.

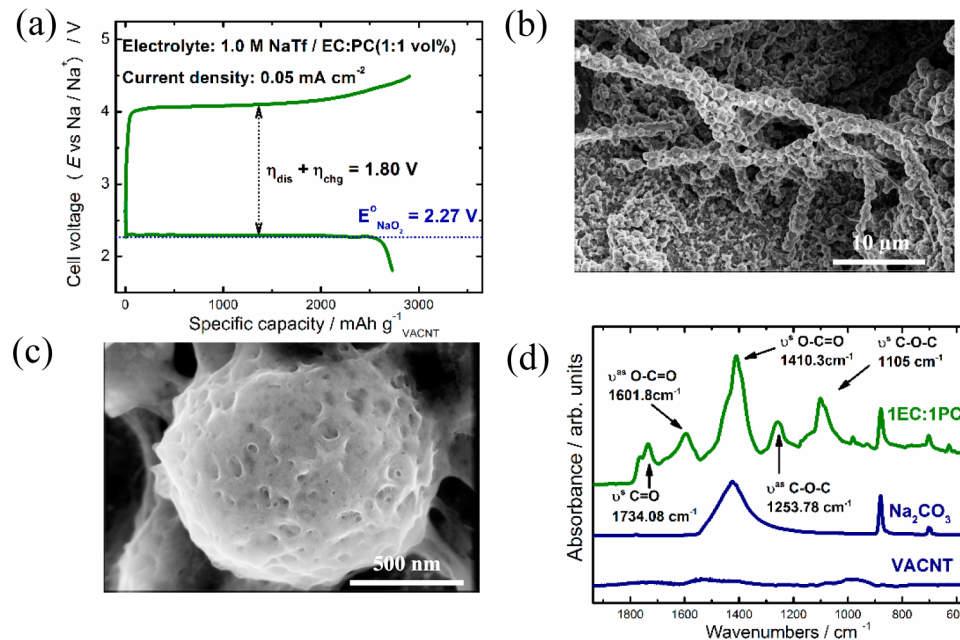


Figure 1. (a) First discharge and charge profile for the Na/EC:PC-NaTf/O₂ cells at the current density of 0.05 mA cm⁻² in voltage range of 1.5–4.5 V; (b-c) SEM images of solid deposit on the VACNT cathodes after the first discharge with the EC/PC electrolyte; (d) FT-IR spectra of the VACNT cathodes after the first discharge, the pristine VACNT, and the standard sample of Na₂CO₃ as the reference.

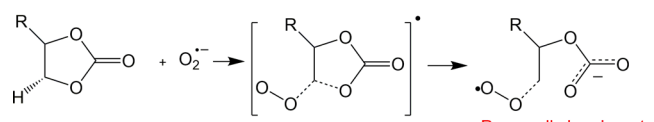
Na—O₂ Batteries with Alkyl Carbonate-Based Electrolytes. The first discharge/charge behavior of the battery with EC/PC electrolyte is investigated. The typical curve measured in potential range of 1.5–4.5 V at the current density of 50 μ A cm⁻² is shown in Figure 1a. The specific capacity is calculated according to the mass of carbon in the VACNT cathodes. It shows a specific discharge capacity of 2800 mAh g⁻¹ and a comparable charge capacity. The voltage hysteresis value is calculated to be 1.8 V if the potential value is extracted from the middle of the plateau. The discharge plateau of 2.29 V is slightly higher than the thermodynamic potential of NaO₂ formation, which implies that other products rather than NaO₂ formed during discharge. Morphological change of VACNTs cathode after discharge is characterized by SEM. As shown in Figure 1b, a large amount of rust-like particles in size of 1 μ m deposit on the nanotube surfaces after the full discharge. With closer observation in Figure 1c, these solid deposits are composed of amorphous species (as confirmed by the absence of peaks in XRD measurement).

Figure 1d shows that the rust-like particles are mainly composed of Na₂CO₃, which agrees with the previous reports.¹⁹ Other peaks can be attributed to O—C=O, C—O, and C—O—C functional groups, which indicates formation of organic products, such as carboxylates, esters, etc. By using this technique, the proportion of NaO₂ after the full discharge in EC/PC cells is found to be as low as 8.92%. If peroxides (Na₂O₂ or Na₂O₂·2H₂O, as shown by previous reports)¹⁶ other than NaO₂ are taken into consideration, the Na₂O₂ yield will be 4.46%. The rest of discharge products was the mixture of sodium carbonate and carboxylate. This indicates that the undesired side-reaction products dominate the discharge products. The side reactions caused by H₂O can be excluded for strictly controlled H₂O contents (\sim 10 ppm) in electrolyte and operating atmosphere (H₂O < 0.1 ppm). As reported in previous researches of Li—O₂ batteries, carbonate-based solvents is highly susceptible to the nucleophilic attack of O₂^{•-}.²³ It can be concluded that the side-reaction products

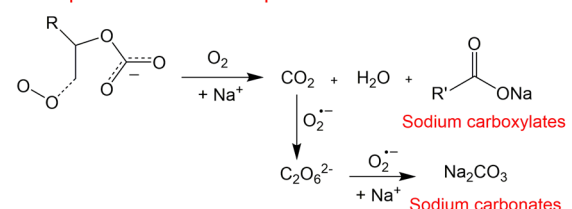
result from the decomposition of carbonate electrolyte. Here, we propose a discharge reaction mechanism for the Na—O₂ batteries with carbonate electrolyte as shown in Scheme 1.^{23,24}

Scheme 1. Proposed Two-Step Mechanism for Decomposition of the EC/PC Solvent during Discharge^a

Step 1: nucleophilic attack



Step 2: oxidative decomposition



^aR stands for H- and CH₃-group of EC and PC, respectively.

The cyclic (or linear) carbonate solvent molecules undergo nucleophilic attack reactions with superoxide radicals or sodium superoxides, which generate peroxyalky carbonates as intermediates. Under further attack of oxygen molecular and radicals, the peroxyalky carbonates decompose to CO₂, H₂O, and carboxylates. Based on the previous investigation, the evolved CO₂ molecular prefers to react with the superoxide radicals to yield C₂O₆²⁻, which is readily decomposed to the sodium carbonate.²⁵

Briefly speaking, the reaction process in Na—O₂ batteries with carbonate solvents is primarily associated with the decomposition of electrolyte solvent rather than the reversible

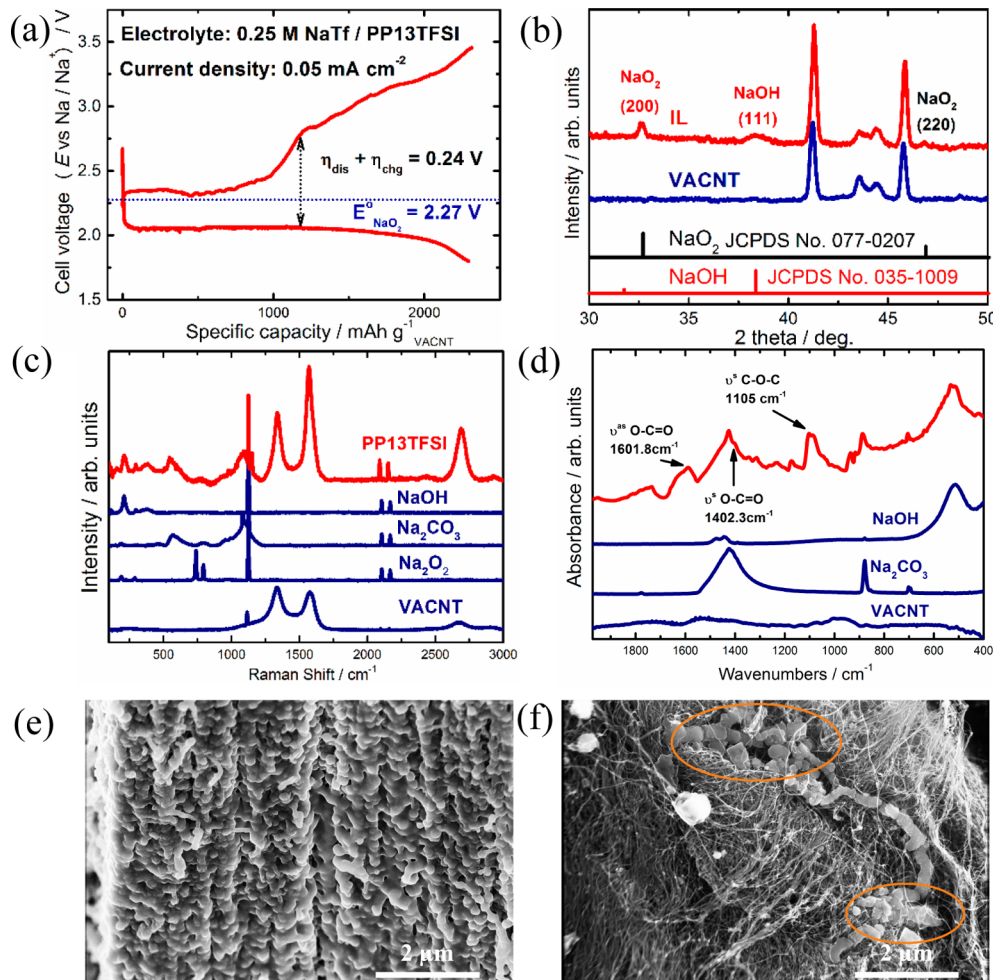


Figure 2. (a) First discharge and charge profile for the typical Na/PP13TFSI-NaTfO₂ cell at the current density 0.05 mA cm⁻² in the voltage range of 1.8–3.45 V. The test temperature of PP13TFSI-based cell is 60 °C; (b) XRD scans on the VACNT cathodes disassembled from the cells with the PP13TFSI-based electrolyte after the first discharge; (c) the Raman and (d) FTIR spectra of the discharged VACNT cathodes from the PP13TFSI-based cells and reference spectra of NaOH, Na₂CO₃, Na₂O₂, and the VACNT before discharge; (e) SEM images for the VACNT cathodes from the PP13TFSI-based cells and (f) morphology of the solid deposits as indicated by the red cycle.

formation and decomposition of NaO₂. This is similar to that of Li–O₂ cells with carbonate-based electrolyte.²³

Na–O₂ Batteries with Ionic-Liquid-Based Electrolytes.

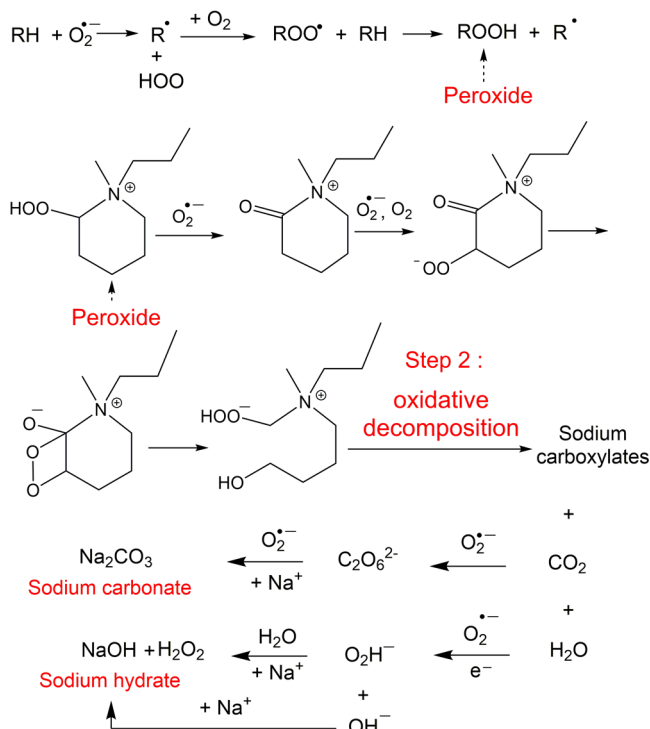
Here, we carry out investigation on the electrochemical performance of the Na–O₂ batteries with the PP13TFSI-based electrolytes, which were frequently used in the Li–O₂ batteries.^{24,26–28} The galvanostatic discharge/charge profiles of the typical Na/PP13TFSI-NaTfO₂ cells measured at the current density of 0.05 mA cm⁻² in potential range of 1.8–3.45 V are displayed in Figure 2a. It can be seen that the discharge capacity is as high as ~2730 mAh g⁻¹ with a voltage plateau similar to that of the TEGDME-based cell. Upon charging, a lower plateau at ~2.29 V and an upper slope from 2.5 to 3.5 V can be observed. In Figure 2b, the weak diffraction peaks of the NaO₂ appear after the first discharge to 1.8 V. The peak at 38.4° can be assigned to NaOH (JCPDS card No. 035-1009), which is consistent with the Raman results, as shown in Figure 2c. Furthermore, the FTIR confirms formation of NaOH and suggests the presence of Na carbonates and Na carboxylates. Correspondingly, two distinct morphologies are observed on discharged VACNT cathodes, as shown in Figure 2e,f. Most nanotubes are densely coated by the ball-shaped products. Interestingly, some cuboid-shaped NaO₂ particles can be found

among the VACNT bundles. The amount of NaO₂ is quantified by chemical titration, which is approximately 38.5% of ORR products. By combining these results with the charging profile, it is reasonable to propose that the lower voltage plateau is related to oxidation of NaO₂ and that the upper slope is related to the decomposition of other products that come from the parasitic reactions between O₂^{•-}/NaO₂ and PP13TFSI-based electrolyte.

Based on the previous reports on the autoxidation of weakly and moderately acidic C–H acids,^{30,31a} we propose a possible mechanism of the superoxide-induced autoxidation of PP13⁺. As shown in Scheme 2, the initial oxidation of PP13⁺ by O₂^{•-} to form piperidinium-peroxide anions as an intermediate is kinetically favorable, as shown in step 1. This is in agreement with the calculation reported by Bryantsev et al.³³ Concerning that the Na–O₂ batteries with the ionic-liquid-based electrolytes were measured at 60 °C instead of room temperature, the hydrogen abstraction reaction is most probably promoted due to the decrease of Gibbs free energy. Therefore, it is reasonable to propose that the peroxides rapidly react with O₂^{•-} to further undergo ring cleavage as indicated in step 2 and step 3.³² Then these ring-opened intermediates are oxidized easily by O₂ and O₂^{•-} with sodium carboxylates, CO₂ and H₂O as the final

Scheme 2. Proposed Mechanism for the Decomposition of PP13TFSI Solvent during Discharge^a

Step 1 : oxygen-assisted nucleophilic attack



^aNote that the RH in step 1 presents the *N*-methyl-*N*-propylpiperidinium (PP13^+) anion and that the H is the proton at α -carbon beside imide group.

products (step 2 in Scheme 2). This is in agreement with the previous results reported by McCloskey et al., which demonstrated that a large amount of CO_2 (~10 mol % of ORR products) and H_2O (~10 mol % of ORR products) were evolved from the MPPTFSI (i.e., PP13TFSI) cell during discharge,^{21c} followed by reaction of CO_2 and H_2O with superoxide radicals with the result of sodium carbonate and sodium hydroxide.

Na–O₂ Batteries with Ether-Based Electrolyte. Figure 3a shows the galvanostatic discharge/charge curve at the current density of 0.05 mA cm^{-2} in potential range of 1.5–3.25 V. It can be seen that the cell exhibits a discharge capacity of 3500 mAh g^{-1} , which is much larger than that with the EC/PC-based electrolyte. More importantly, we observed a voltage plateau of 2.05 V during discharge and 2.29 V during charge, corresponding to an overpotential ($\eta_{\text{dis}} + \eta_{\text{chg}}$) of 240 mV and an electrical energy efficiency of 90%.

To identify the discharge products, XRD measurement was conducted on the discharged cathodes from Na–O₂ batteries with the TEGDME-based electrolyte. Figure 3b indicates that the peaks appearing after the first discharge agree well with the referred diffraction patterns of sodium superoxide (JCPDS No. 01-077-0207). SEM images show a large amount of cuboid particles in size of $\sim 1\text{--}2 \mu\text{m}$ (Figure 3c,d), which can be confirmed as NaO₂ by energy dispersive spectroscopy (EDS) analysis (Figure S1, Supporting Information). The accurate amount of NaO₂ determined by chemical titration was up to 92.8% of oxygen reduction reaction (ORR) products. The rest 7.2% of the discharge capacity should be attributed to the

undesired side-reactions. As shown in Figure 3d, the byproducts grow as the amorphous-like film coated on surface of carbon nanotubes in the vicinity of NaO₂ particles. Raman and FTIR spectra provide more information on the composition of these amorphous films. From Figure 3e, the intense Raman peak located at 1154 cm^{-1} indicates NaO₂ as the main discharge product,¹³ which is clearly observed in Figure S2, Supporting Information. Compared to the spectra of standard samples, other peaks can be assigned to sodium carbonate (Na_2CO_3). Furthermore, FTIR spectroscopy (Figure 3f) reveals existence of carboxylates species ($\text{O}=\text{C}-\text{O}$ asymmetric stretch in 1601 cm^{-1} band and symmetric stretch in 1406 cm^{-1} band) and esters ($\text{C}-\text{O}-\text{C}$ asymmetric stretch in 1105 cm^{-1}).³³

Based on the calculation done by Bryantsev et al.,³⁰ the direct oxidation of ether molecular by $\text{O}_2^{\bullet-}$ and NaO₂ is difficult since this reaction is endothermic, which demands a high activation energy. Nevertheless, the ether is found to undergo slow oxidation under oxidizing atmosphere.^{34,35} Although the oxidation of TEGDME by O₂ molecular is an endothermic process, hydroperoxide formation in the autoxidation process, as shown in step 1 in Scheme 3, is highly reactive with superoxide, generating more reactive species such as esters. Furthermore, esters are easily decomposed into the materials with higher stability, such as carboxylates and CO₂ as depicted in step 2. This mechanism is consistent with the recent theoretical study.³⁶ As mentioned above, the side reaction only contributes 7.2% of the overall discharge capacity, indicating that the TEGDME is a relatively stable solvent for the Na–O₂ battery.

Correlation between NaO₂ Yield and Acidity of Solvent. The above discussion indicates that the sodium carbonate (Na_2CO_3) and sodium carboxylates ($\text{R}-\text{C}=\text{O}-\text{ONa}$) are the dominant discharge products in the EC/PC-based cells. The ionic liquid PP13TFSI leads to a large amount of side-products including carbonate and hydroxide species while small amount of NaO₂ after discharge. In contrast, the sodium superoxide (NaO₂) is the major discharge product in the TEGDME-based cells. Obviously, the solvent stability significantly influence the cell chemistry of NaO₂ during discharge. Understanding the relationship between solvent property and stability against superoxide is critical for the selection and design of stable electrolytes for the Na–O₂ batteries. Based on the extensive research on the organic chemistry of O₂^{•-} in aprotic media, C–H acidity of solvents is one important parameter influencing the reaction between this solvent and O₂^{•-}. C–H acidity is determined by its acid dissociation constant, pK_a . To examine whether this is also the case here, the pK_a analysis of the electrolyte solvent is carried out, as described in the Experimental Section and Supporting Information.

As shown in Supporting Information, the pK_a of EC/PC (~20.9) and PP13TFSI (~30) is relatively low, which correlates with the lower yields of NaO₂ in EC/PC- and PP13TFSI-based cells. While the larger value of pK_a (~46–52)^{31a} with respect to TEGDME leads to a higher yield of NaO₂ in the TEGDME-based cells. As discussed in the previous papers,^{29a,b} the certain amount of H₂O, either existing as trace (~10 ppm) in the electrolyte or the reaction-formed H₂O, may promote the electrochemical formation of NaO₂ and thus improve the discharge capacities. Correlation between the NaO₂ yield and the pK_a value is plotted in Figure 4, which shows a linear relationship. Note that the yield of NaO₂ is

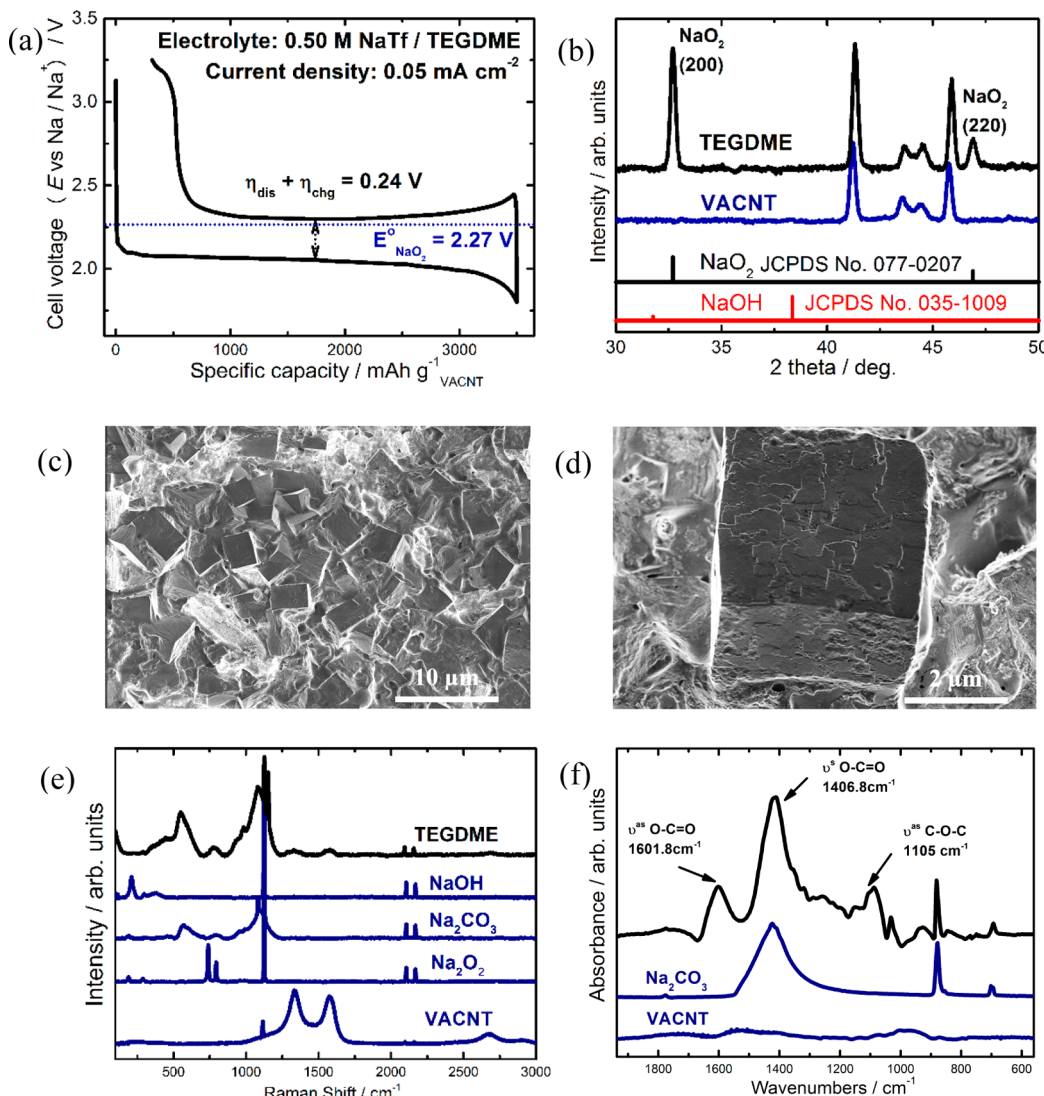


Figure 3. (a) First discharge and charge curve for the typical Na/TEGDME-NaTf/O₂ cell at the current density of 0.05 mA cm⁻² in the voltage range of 1.8–3.25 V; (b) XRD scans on the VACNT cathodes from the cells with the TEGDME-based electrolytes after the first discharge; (c) SEM image for the VACNT cathode from the TEGDME-based cells and (d) morphology of the solid deposits; (e) Raman and (f) FTIR spectra of the discharged VACNT cathode from the TEGDME-based cell and reference spectra of NaOH, Na₂CO₃, Na₂O₂, and the pristine VACNT.

defined as the amount of NaO₂ produced divided by the amount of NaO₂ expected given the Coulometry as referred to in ref 21a. Concerning that there exists a large amount of side discharge products other than NaO₂ in the case of EC/PC and ionic-liquid-based electrolytes, the calculated yield of NaO₂ gives the upper limit value. Though there exists obvious error in the case of EC/PC- and ionic-liquid-based electrolytes, the results here clearly indicate that the solvent with the larger pK_a value corresponds to the better stability against O₂^{•-} attack, which is also beneficial to improvement of the electrical energy efficiency of the Na–O₂ batteries.

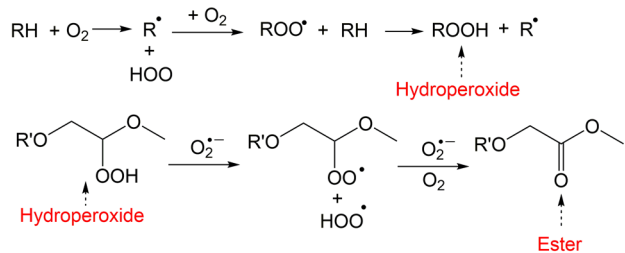
CONCLUSIONS

To gain a deeper insight into the stability issue of nonaqueous electrolytes in the Na–O₂ batteries, a comparative study has been carried out in terms of the correlation between the yield of demanded NaO₂ and the acid dissociation constant (pK_a) of solvent.^{31b} By combining qualitative spectroscopic analysis and quantitative chemical titration, solid discharge products deposited on VACNT cathode after discharge in the three

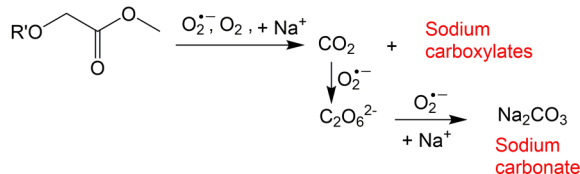
representative electrolytes were systematically investigated. It is found that the desired NaO₂ product is uneasy to be detected in the Na–O₂ batteries with the carbonate-based electrolytes (EC/PC with pK_a of ~20.9) because of its low ratio in the discharge product (8.92%). Instead, the final discharge products primarily consist of Na₂CO₃ coupled with sodium alkyl-carboxylate, which accounts for more than 90% of the final deposits. The ionic liquid (PP13TFSI, pK_a ≈ 30) used as the electrolyte solvent for the Na–O₂ battery has been studied for the first time. However, sole 38.5% of the solid deposit after discharge is NaO₂, and the rest consists of sodium carbonate, sodium carboxylate, and sodium hydroxide as parasitic products, and 92.7% of the total discharge deposit is NaO₂ in the cells based on the ether-based electrolytes (TEGDME with pK_a of ~46–52), owing to its good stability. It can be concluded that a high value of pK_a is beneficial to solvent stability and thus helpful for improving round-trip energy efficiency of the Na–O₂ battery.

Scheme 3. Proposed Mechanism for Evolution of Ether-Based Solvent during Discharge^a

Step 1 : oxygen-assisted nucleophilic attack



Step 2 : oxidative decomposition



^aNote that the RH in step 1 represents the TEGDME and that the H is the proton at α -carbon beside ethereal group. R' represents the rest part of TEGDME hydroperoxide.

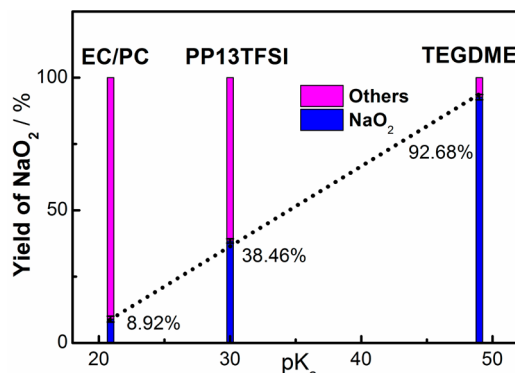


Figure 4. Correlation between NaO₂ yield and acidity of solvent. The yield of NaO₂ is defined as the amount of NaO₂ produced divided by the amount of NaO₂ expected given the Coulometry as referred to in ref 21a. Concerning that there exists a large amount of side discharge products other than NaO₂ in the case of EC/PC- and ionic-liquid-based electrolytes, the calculated yield of NaO₂ gives the upper limit value.

ASSOCIATED CONTENT

Supporting Information

The Supporting Information is available free of charge on the ACS Publications website at DOI: [10.1021/acs.jpcc.5b09187](https://doi.org/10.1021/acs.jpcc.5b09187).

EDS, Raman spectra, pK_a determination, and first discharge and charge profiles ([PDF](#))

AUTHOR INFORMATION

Corresponding Author

*Tel: 0086-21-52411032. Fax: 0086-21-52411802. E-mail: xxguo@mail.sic.ac.cn.

Notes

The authors declare no competing financial interest.

ACKNOWLEDGMENTS

The authors would like to acknowledge the financial supports from National Key Basic Research Program of China (Grant No. 2014CB921004), Key Research Program of Chinese Academy of Sciences (Grant No. KGZD-EW-T06), and National Natural Science Foundation of China (Grant No. U1232111).

REFERENCES

- Bruce, P. G.; Freunberger, S. A.; Hardwick, L. J.; Tarascon, J. M. Li-O₂ and Li-S Batteries with High Energy Storage. *Nat. Mater.* **2011**, *11*, 19–29.
- Dunn, B.; Kamath, H.; Tarascon, J. M. Electrical Energy Storage for the Grid: A Battery of Choices. *Science* **2011**, *334*, 928–935.
- (a) Lee, J. S.; Tai Kim, S.; Cao, R.; Choi, N. S.; Liu, M.; Lee, K. T.; Cho, J. Metal-Air Batteries with High Energy Density: Li-Air Versus Zn-Air. *Adv. Energy Mater.* **2011**, *1*, 34–50. (b) Shiga, T.; Hase, Y.; Kato, Y.; Inoue, M.; Takechi, K. A Rechargeable Nonaqueous Mg-O₂ Battery. *Chem. Commun.* **2013**, *49*, 9152–9154.
- (a) Yadegari, H.; Banis, M. N.; Xiao, B. W.; Sun, Q.; Li, X.; Lushington, A.; Wang, B. Q.; Li, R. Y.; Sham, T. K.; Cui, X. Y.; Sun, X. L. Three-Dimensional Nanostructured Air Electrode for Sodium-Oxygen Batteries: A Mechanism Study toward the Cyclability of the Cell. *Chem. Mater.* **2015**, *27*, 3040–3047. (b) Yadegari, H.; Li, Y. L.; Norouzi Banis, M.; Li, X. F.; Wang, B. Q.; Sun, Q.; Li, R. Y.; Sham, T. K.; Cui, X. Y.; Sun, X. L. *Energy Environ. Sci.* **2014**, *7*, 3747–3757.
- (c) Sun, Q.; Hosseini, Y.; Norouzi Banis, M.; Li, J.; Xiao, B. W.; Wang, B. Q.; Lawes, S.; Li, X.; Li, R. Y.; Sun, X. L. Self-stacked nitrogen-doped carbon nanotubes as long-life air electrode for sodium-air batteries: Elucidating the evolution of discharge product morphology. *Nano Energy* **2015**, *12*, 698–708. (d) Li, Y. L.; Yadegari, H.; Li, X. F.; Norouzi Banis, M.; Li, R. Y.; Sun, X. L. Superior Catalytic Activity of Nitrogen-Doped Graphene Cathode for High Energy Capacity Sodium-Air Batteries. *Chem. Commun.* **2013**, *49*, 11731–11733.
- Kim, H.; Jeong, G.; Kim, Y. U.; Kim, J. H.; Park, C.-M.; Sohn, H.-J. Metallic Anodes for Next Generation Secondary Batteries. *Chem. Soc. Rev.* **2013**, *42*, 9011–9034.
- Abraham, K. M.; Jiang, Z. A Polymer Electrolyte-Based Rechargeable Lithium/Oxygen Battery. *J. Electrochem. Soc.* **1996**, *143*, 1–5.
- Girishkumar, G.; McCloskey, B.; Luntz, A. C.; Swanson, S.; Wilcke, W. Lithium-Air Battery: Promise and Challenges. *J. Phys. Chem. Lett.* **2010**, *1*, 2193–2203.
- Black, R.; Adams, B.; Nazar, L. F. Nonaqueous and Hybrid Li-O₂ Batteries. *Adv. Energy Mater.* **2012**, *2*, 801–815.
- Kraytsberg, A.; Ein-Eli, Y. Review on Li-Air Batteries: Opportunities, Limitations and Perspective. *J. Power Sources* **2011**, *196*, 886–893.
- Zhao, N.; Li, C. L.; Guo, X. X. Review of Methods for Improving the Cyclic Stability of Li-Air Batteries by Controlling Cathode Reactions. *Energy Technology* **2014**, *2*, 317–324.
- (a) Fan, W. G.; Guo, X. X.; Xiao, D. D.; Gu, L. Influence of Gold Nanoparticles Anchored to Carbon Nanotubes on Formation and Decomposition of Li₂O₂ in Nonaqueous Li-O₂ Batteries. *J. Phys. Chem. C* **2014**, *118*, 7344–7350. (b) Fan, W. G.; Cui, Z. H.; Guo, X. X. Tracking Formation and Decomposition of Abacus-Ball-Shaped Lithium Peroxides in Li-O₂ Cells. *J. Phys. Chem. C* **2013**, *117*, 2623–2627.
- Cui, Z. H.; Guo, X. X. Manganese Monoxide Nanoparticles Adhered to Mesoporous Nitrogen-Doped Carbons for Nonaqueous Lithium-Oxygen Batteries. *J. Power Sources* **2014**, *267*, 20–25.
- Hartmann, P.; Bender, C. L.; Vračar, M.; Dürr, A. K.; Garsuch, A.; Janek, J.; Adelhelm, P. A Rechargeable Room-Temperature Sodium Superoxide (NaO₂) Battery. *Nat. Mater.* **2012**, *12*, 228–232.
- Hartmann, P.; Bender, C. L.; Sann, J.; Durr, A. K.; Jansen, M.; Janek, J.; Adelhelm, P. A Comprehensive Study on the Cell Chemistry of the Sodium Superoxide (NaO₂) Battery. *Phys. Chem. Chem. Phys.* **2013**, *15*, 11661–11672.

- (15) Peled, E.; Golodnitsky, D.; Mazor, H.; Goor, M.; Avshalomov, S. Parameter Analysis of a Practical Lithium- and Sodium-Air Electric Vehicle Battery. *J. Power Sources* **2011**, *196*, 6835–6840.
- (16) Sun, Q.; Yang, Y.; Fu, Z. W. Electrochemical Properties of Room Temperature Sodium–Air Batteries with Nonaqueous Electrolyte. *Electrochim. Commun.* **2012**, *16*, 22–25.
- (17) Liu, W.; Sun, Q.; Yang, Y.; Xie, J. Y.; Fu, Z. W. An Enhanced Electrochemical Performance of Sodium–Air Battery with Graphene Nanosheets as Air Electrode Catalysts. *Chem. Commun.* **2013**, *49*, 1951–1953.
- (18) (a) Kim, J.; Lim, H. D.; Gwon, H.; Kang, K. Sodium–Oxygen Batteries with Alkyl-Carbonate and Ether Based Electrolytes. *Phys. Chem. Chem. Phys.* **2013**, *15*, 3623–3629.
- (19) Zhao, N.; Li, C. L.; Guo, X. X. Long-Life Na-O₂ Batteries with High Energy Efficiency Enabled by Electrochemically Splitting NaO₂ at Low Overpotential. *Phys. Chem. Chem. Phys.* **2014**, *16*, 15646–15652.
- (20) Matthews, W. S.; Bares, J. E.; Bartmess, J. E.; Bordwell, F. G.; Cornforth, F. J.; Drucker, G. E.; Margolin, Z.; McCallum, R. J.; McCollum, G. J.; Vanier, N. R. Equilibrium acidities of carbon acids. VI. Establishment of an absolute scale of acidities in dimethyl sulfoxide solution. *J. Am. Chem. Soc.* **1975**, *97* (24), 7006–7014.
- (21) (a) McCloskey, B. D.; Valery, A.; Luntz, A. C.; Gowda, S. R.; Wallraff, G. M.; Garcia, J. M.; Mori, T.; Krupp, L. E. Combining Accurate O₂ and Li₂O₂ Assays to Separate Discharge and Charge Stability Limitations in Nonaqueous Li–O₂ Batteries. *J. Phys. Chem. Lett.* **2013**, *4* (17), 2989–2993. (b) McCloskey, B. D.; Garcia, J. M.; Luntz, A. C. Chemical and Electrochemical Differences in Nonaqueous Li–O₂ and Na–O₂ Batteries. *J. Phys. Chem. Lett.* **2014**, *5* (7), 1230–1235. (c) McCloskey, B. D.; Bethune, D. S.; Shelby, R. M.; Mori, T.; Scheffler, R.; Speidel, A.; Sherwood, M.; Luntz, A. C. Limitations in Rechargeability of Li–O₂ Batteries and Possible Origins. *J. Phys. Chem. Lett.* **2012**, *3* (20), 3043–304.
- (22) (a) Laoire, C. O.; Mukerjee, S.; Abraham, K. M. Influence of Non-aqueous Solvents on the Electrochemistry of Oxygen in the Rechargeable Lithium–Air Battery. *J. Phys. Chem. C* **2010**, *114*, 9178–9186. (b) Laoire, C. O.; Mukerjee, S.; Plichta, E. J.; Hendrickson, M. A.; Abraham, K. M. Rechargeable Lithium/TEGDME-LiPF₆/O₂ Battery. *J. Electrochim. Soc.* **2011**, *158*, A302–A308. (c) Abraham, K. M.; Jiang, Z.; Carroll, B. Highly Conductive PEO-like Polymer Electrolytes. *Chem. Mater.* **1997**, *9*, 1978–1988. (d) Allen, C. J.; Hwang, J.; Kautz, R.; Mukerjee, S.; Plichta, E. J.; Hendrickson, M. A.; Abraham, K. M. Oxygen Reduction Reactions in Ionic Liquids and the Formulation of a General ORR Mechanism for Li–Air Batteries. *J. Phys. Chem. C* **2012**, *116*, 20755–20764. (e) Peng, Z. Q.; Freunberger, S. A.; Chen, Y. H.; Bruce, P. G. A Reversible and Higher-Rate Li–O₂ Battery. *Science* **2012**, *337*, 563–6.
- (23) Freunberger, S. A.; Chen, Y.; Peng, Z.; Griffin, J. M.; Hardwick, L. J.; Bardé, F.; Novák, P.; Bruce, P. G. Reactions in the Rechargeable Lithium–O₂ Battery with Alkyl Carbonate Electrolytes. *J. Am. Chem. Soc.* **2011**, *133*, 8040–8047.
- (24) Takechi, K.; Higashi, S.; Mizuno, F.; Nishikoori, H.; Iba, H.; Shiga, T. Stability of Solvents against Superoxide Radical Species for the Electrolyte of Lithium–Air Battery. *ECS Electrochem. Lett.* **2012**, *1*, A27–A29.
- (25) Roberts, J. L.; Calderwood, T. S.; Sawyer, D. T. Nucleophilic oxygenation of carbon dioxide by superoxide ion in aprotic media to form the peroxydicarbonate(2-) ion species. *J. Am. Chem. Soc.* **1984**, *106*, 4667–4670.
- (26) Allen, C. J.; Mukerjee, S.; Plichta, E. J.; Hendrickson, M. A.; Abraham, K. M. Oxygen Electrode Rechargeability in an Ionic Liquid for the Li–Air Battery. *J. Phys. Chem. Lett.* **2011**, *2*, 2420–2424.
- (27) Mizuno, F.; Nakanishi, S.; Shirasawa, A.; Takechi, K.; Shiga, T.; Nishikoori, H.; Iba, H. Design of Nonaqueous Liquid Electrolytes for Rechargeable Li–O₂ Batteries. *Electrochemistry* **2011**, *79*, 876–881.
- (28) Cui, Z. H.; Fan, W. G.; Guo, X. X. Lithium–Oxygen Cells with Ionic-Liquid-Based Electrolytes and Vertically Aligned Carbon Nanotube Cathodes. *J. Power Sources* **2013**, *235*, 251–255.
- (29) (a) Xia, C.; Black, R.; Fernandes, R.; Adams, B.; Nazar, L. F. *Nat. Chem.* **2015**, *7*, 496–501. (b) Sun, Q.; Yadegari, H.; Norouzi Banis, M.; Liu, J.; Xiao, B.; Li, X.; Langford, C.; Li, R. Y.; Sun, X. L. *J. Phys. Chem. C* **2015**, *119*, 13433–13441.
- (30) Bryantsev, V. S.; Faglioni, F. Predicting Autoxidation Stability of Ether- and Amide-Based Electrolyte Solvents for Li–Air Batteries. *J. Phys. Chem. A* **2012**, *116*, 7128–7138.
- (31) (a) Bryantsev, V. S. Predicting the stability of aprotic solvents in Li–air batteries: pK_a calculations of aliphatic C–H acids in dimethyl sulfoxide. *Chem. Phys. Lett.* **2013**, *558*, 42–47. (b) Giordani, V.; Bryantsev, V. S.; Uddin, J.; Walker, W.; Chase, G. V.; Addison, D. N-methylacetamide as an Electrolyte Solvent for Rechargeable Li–O₂ Batteries: Unexpected Stability at the O₂ electrode. *ECS Electrochem. Lett.* **2014**, *3*, A11–A14.
- (32) Collins, C. M.; Sotiriou-Leventis, C.; Canalias, M. T.; Leventis, N. A Cyclic Voltammetric Study of the Proton Abstraction from Selected Aromatic Ketones by Superoxide. *Electrochim. Acta* **2000**, *45*, 2049–2059.
- (33) Andrews, L. Infrared Spectra and Bonding in the Sodium Superoxide and Sodium Peroxide Molecules. *J. Phys. Chem.* **1969**, *73*, 3922–3928.
- (34) Di Tommaso, S.; Rotureau, P.; Crescenzi, O.; Adamo, C. Oxidation Mechanism of Diethyl Ether: A Complex Process for a Simple Molecule. *Phys. Chem. Chem. Phys.* **2011**, *13*, 14636–14645.
- (35) Naito, M.; Radcliffe, C.; Wada, Y.; Hoshino, T.; Liu, X.; Arai, M.; Tamura, M. A Comparative Study on the Autoxidation of Dimethyl Ether (DME) Comparison with Diethyl Ether (DEE) and Diisopropyl Ether (DIPE). *J. Loss Prev. Process Ind.* **2005**, *18*, 469–473.
- (36) Bryantsev, V. S.; Giordani, V.; Walker, W.; Blanco, M.; Zecevic, S.; Sasaki, K.; Uddin, J.; Addison, D.; Chase, G. V. Predicting Solvent Stability in Aprotic Electrolyte Li–Air Batteries: Nucleophilic Substitution by the Superoxide Anion Radical (O₂^{•-}). *J. Phys. Chem. A* **2011**, *115*, 12399–12409.